Preliminary fractal analysis of fracture spacing inferred from an acoustic televiewer log run in the Basel-1 geothermal well...

Conference Paper · August 2016

CITATIONS
0

READS
18

3 authors, including:

Benoît Valley
Université de Neuchâtel
60 PUBLICATIONS **388** CITATIONS
SEE PROFILE

Martin Ziegler
ETH Zurich
14 PUBLICATIONS **21** CITATIONS
SEE PROFILE

Rock Mechanics and Rock Engineering: From the Past to the Future – Ulusay et al. (Eds)
© 2016 Taylor & Francis Group, London, ISBN 978-1-138-03265-1

Preliminary fractal analysis of fracture spacing inferred from an acoustic televiewer log run in the Basel-1 geothermal well (Switzerland)

M.J.A. Moein
Geological Institute, ETH Zurich, Switzerland

B. Valley
Center for Hydrogeology and Geothermics, University of Neuchâtel, Switzerland

M. Ziegler
Geological Institute, ETH Zurich, Switzerland

ABSTRACT: Development of a geological model for an Enhanced Geothermal System (EGS) reservoir requires a characterization of the fracture network. Previous studies have identified fractures from an acoustic image log run in the crystalline basement section of the Basel-1 well and described fracture sets and fracture zone characteristics. Using the Cantor's Dust method, we investigated the fractal behavior of four major natural fracture sets intersected by the Basel-1 well. These sets are differently distributed between 2600 m and 5000 m (i.e., the logged depth) along the well below the rotary table of the rig. The obtained fractal dimensions (D) vary between 0.35 and 0.60 for the four fracture sets. Similar D values ranging for sets 1–3 in the interval between 2600 m and 3000 m emphasize the role of the geological setting in the distribution of fractures. Moreover, the spacing distribution of sets 2 and 3 show a clear power-law distribution.

1 INTRODUCTION

An Enhanced Geothermal System (EGS) seeks at extracting heat from deep underground by circulating a fluid between injection and production wells. In most EGS projects, fluid flow occurs essentially along fractures as the matrix permeability is small (Genter et al. 2010). In general, the low permeability of such reservoirs prevents production at economical rates. The enhancement of fracture permeability to facilitate fluid circulation is required. One approach to enhance and create the permeability is to perform hydraulic stimulations. In order to design and assess EGS reservoir stimulation strategies, development of a geological model with representation of lithological domains and characterization of the fracture network is required. This characterization includes a correct statistical distribution of fractures and fracture set properties. Such a geological model is crucial for geomechanical simulations during the life-time of an EGS reservoir, too.

The existence of fractures within the target EGS rock mass plays a controlling role on the mechanical behavior during reservoir stimulation. Valley and Evans (2007) have identified more or less continuous, local stress variations from analyzing wellbore failures along deep wells at the Soultz-sous-Forêts EGS in France, and attributed these stress changes to the existence of natural fractures cut by the deep boreholes. Similar observations were made at the Basel EGS project in Switzerland (Valley and Evans 2009).

This paper aims at studying the distribution of fracture spacing in the crystalline basement section below Basel that was penetrated by the Basel-1 well. Knowledge of the spacing distribution is a crucial step towards populating a reservoir model with synthetic fractures consistent with the observations obtained from deep boreholes. For our analysis we used the fracture data from Ziegler et al. (2015). Ziegler et al. (2015) have characterized the natural fractures and fracture zones characteristics (location, orientation, set spacing, fracture zone thickness and internal structure) in the crystalline basement ("Deep Heat Mining" project, Switzerland).The analysis was performed using an acoustic televiewer log and other logging data (e.g., bulk density and p-wave velocity). For a complete description of the dataset and interpretation methodology we refer to Ziegler et al. (2015).

Amongst the various fracture attributes such as persistence, spacing, aperture etc., this study focuses on analyzing the spacing distribution of fractures using fractal geometry. A fractal analysis of fracture intersections with the borehole is expected to improve our understanding of the distribution of fractures in the crystalline basement. We aim at quantifying the

fractal dimension of fracture sets spacing in the crystalline basement along the Basel-1 well using the Cantor's Dust method. We also studied the statistical distribution of fracture spacing in different sets to find any probable power-law distributions. The relation between the power law exponents and fractal dimensions is discussed, too.

2 FRACTAL BEHAVIOR OF FRACTURES

The fractal geometry is a branch of mathematics that deals with the quantification of repeating patterns on different scales. Fractals have been widely used in different areas of geoscience to understand these patterns. Using this geometry, it is possible to quantify the scaling of fracture attributes. In addition, it has been used to cluster earthquakes and quantify induced seismicity (Smalley et al. 1987, Enescu and Ito 2001, Hainzl 2004). Scaling and spatial clustering of fractures are important parameters that control the organization of the flow within a fractured rock reservoir. Barton and Zoback (1992) have suggested that the self-similarity of fractures in the Earth's crust exists on a very wide range of scales ranging from millimeters to hundreds of meters. Self-similar distributions show scale invariant characteristics. There are numerous observations in the literature reporting the fractal behavior of different fracture attributes such as trace length, spacing, RQD (Rock Quality Designation, Deere and Deere (1988)), aperture, surface roughness etc. (Velde et al. 1990, Power and Tullis 1991, Barton and Zoback 1992, Boadu and Long 1994).

3 FRACTAL ANALYSIS OF FRACTURES INTERSECTING A BOREHOLE

The intersection of fracture planes with a borehole centerline can be represented as points along a single dimension. If the distribution of fracture intersections follows a fractal behavior, the following equation will be valid for all r:

$$N = c \cdot r^{-D} \quad (1)$$

where N is the number of divisions that cover all of the fractures in equally spaced divisions of length r, D is the fractal dimension, and c is a constant. The fractal dimension D is in the range $0 < D < 1$. Here, we will apply the Cantor's Dust method to obtain the fractal dimension of different fracture sets intersecting the borehole.

3.1 *Cantor's Dust method (Cantor 1872)*

This method tries to cover the intersection of fracture planes with the borehole by successively smaller intervals in each step. If the fracture intersections in a set follow a fractal distribution, the number of intervals containing fractures follow a linear trend with slope m on a log-log plot. The slope m of this line equals to $1–D$. A detailed description to obtain fractal dimensions with the *Cantor's Dust* method is given by Velde et al. (1991).

3.2 *Power-law statistical distributions*

It is assumed that the true spacing of fractures in specific sets follows a power-law distribution. Valley (2007) has studied different statistical parameters using different distributions for different fracture sets in the Soultz-Sous-Forêts EGS. He has extracted power-law exponents for different sets by fitting a line to the linear section of plots showing *log(cumulative number)* vs. *log(spacing)* and obtained a wide range of exponents ranging between 0.63 and 1.06 for four fracture sets in the GPK3 and GPK4 wells. While log-normal distribution shows a better fit to the spacing distributions derived from borehole imaging at Soultz (both wells), the spacing distribution obtained from core fracture logs shows a better fit to the power-law distribution (Genter et al. 1997). This deviation is mainly due to the bias imposed by the censoring effect. The censoring effect is due to the resolution limit where short fractures are not completely observed (Bonnet et al. 2001). Moreover, the spacing might be influenced by truncation effect due to incomplete sampling of long fractures.

4 GEOLOGICAL SETTING AND AVAILABLE DATASETS

The crystalline section below Basel was penetrated by the Basel-1 well between 2507 m and 5000 m (all depths given in this article are measured along hole from the rotary table). A total of 1164 natural fractures (certain and uncertain) were identified in the logged interval between 2600 m and 5000 m (Ziegler et al. 2015, Fig. 1). Out of these, 1035 fractures were grouped into six possible sets based on their orientation. Some of the sets may be conjugate pairs. In this study we do not take the uncertainty rating into account and studied all fractures that were grouped into the largest sets 1–4. The number of fractures in sets 5 and 6 is too small to perform a statistical study. The number of fractures in different sets and their mean orientation (dip direction and dip angle) are listed in Table 1. The distribution of four fracture sets along the borehole is displayed in Figure 1a, while Figure 1b and 1c show the p-wave velocity and smoothed density. It can be seen that the fracture frequency in the first 400 m is distinctly higher than in the rest of the borehole and p-wave velocity is less. This was suggested to likely reflect a paleo-weathered zone since the interface with the sediments lies at ~2507 m (Ziegler et al. 2015).

5 RESULTS

5.1 *Cantor's Dust method analysis*

Table 2 summarizes the results of fractal dimensions using Cantor's Dust method (see section 3.1). Set 4 has

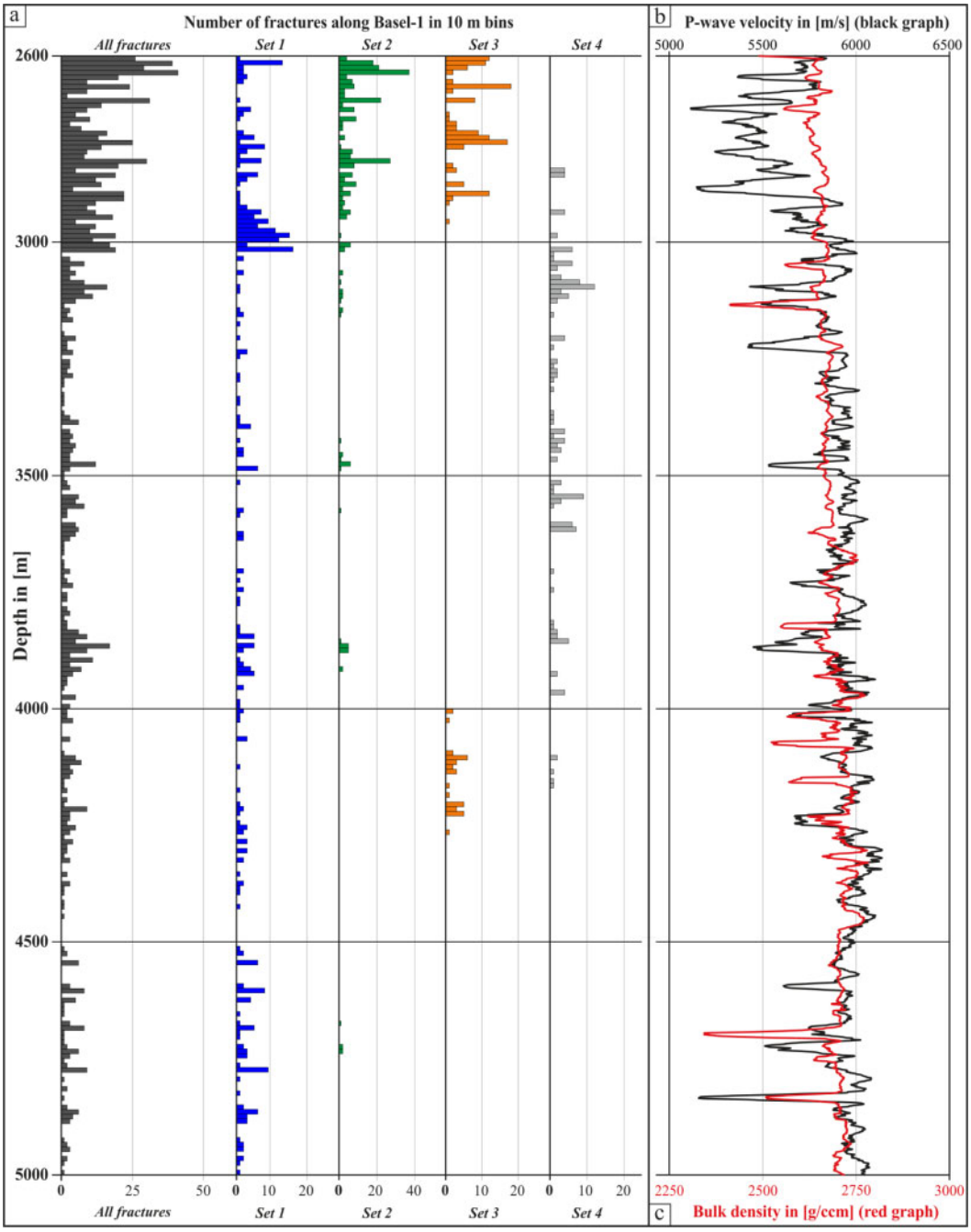

Figure 1. a) Histograms of all fractures (1164 fractures) and set 1–4 vs. depth in 10 m bins. b) Smoothed p-wave velocity versus depth using a moving average filter with a window length of 100 m. c) Smoothed density log using a moving average filter with a window length of 100 m.

the highest *D* value, while set 3 has the lowest. Set 3 occurs in two intervals, between about 2600–2957 m and 4000–4261 m (Fig. 1a).The fractal analysis of the different intervals shows different fractal dimensions of 0.45 (2600–2957 m) and 0.59 (4000–4261 m) for set 3 (Table 3). This might be due to the slightly different geological context for these two intervals: the upper interval is located within the more fractured section of the rock mass presenting also lower p-wave velocity (see Fig. 1b) while the lower interval is located at a depth with smaller fracture density and no velocity anomaly. Indeed, the first 400 m interval reflects a

Table 1. Number of fractures in sets and fracture set mean orientation.

Fracture set	Number of fractures	Mean dip direction [°]	Mean dip angle [°]
1	348	250	66
2	297	62	62
3	173	195	61
4	152	308	68

Table 2. Fractal dimension of sets 1–4 along the Basel-1 well.

Fracture set	*D* [–]
1	0.54
2	0.48
3	0.35
4	0.60

Table 3. Fractal dimension of set 3 in different intervals.

Fracture set	*D* [–]
1	0.54
2	0.48
3	0.35
4	0.60

Table 4. Fractal dimension of different sets in the top 400 m of the logged section.

Fracture set	*D* [–]
1	0.46
2	0.44
3	0.45

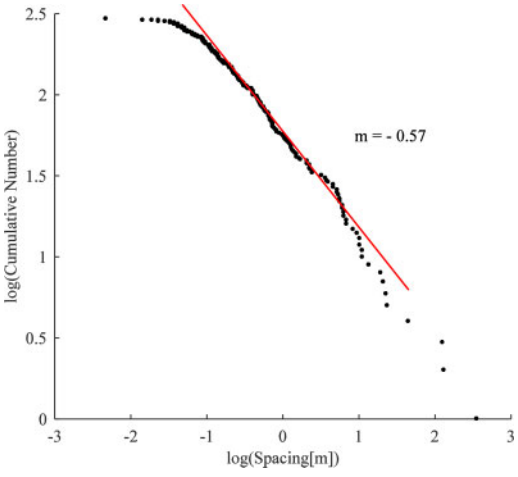

Figure 2. True spacing distribution of set 2 showing a clear power-law distribution.

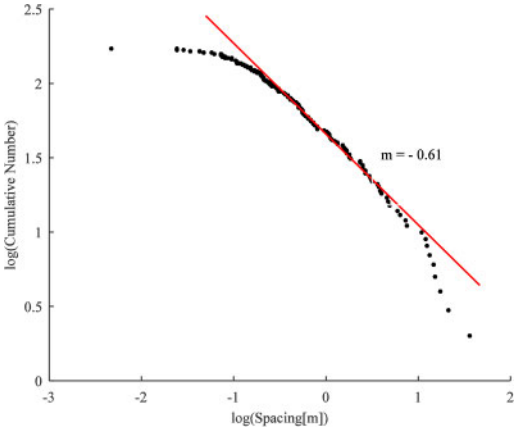

Figure 3. True spacing distribution of set 3 showing a power-law distribution for more than 2 orders of magnitude.

rock mass which is different from deeper sections (see section 4). The fractal dimensions of sets 1–3 in this interval are reported in (only a few fractures of set 4 occur in the interval 2600–3000 m). The similar *D* values suggest the same distribution for the three fracture sets in the top 400 m of the logged section. At least, set 1 and set 2 may be a conjugate pair conform to the Hercynian direction (i.e., striking NW). This might reflect the same origin of the fractures.

5.2 *Power-law distribution of spacing*

The exponent of power-law distribution of fracture spacing were determined similarly to Valley (2007) (see section 3.2). For this analysis, we computed true fracture spacing by considering the mean set orientation which is oblique to the borehole and correcting the spacing measured along the borehole. Although the spacing distributions are not entirely linear on a log-log plot, the linearity was sufficient for sets 2 and 3 over about two orders of magnitude. We picked the longest range of spacing with linear distribution and determined its slope m (Fig. 2 and 3). According to the discussion in section 3.2, the observed spacing distribution is affected by the censoring and truncation effects. For set 2 and 3, there is a good agreement between the power-law exponents and the fractal dimension (actually 1–*D*) obtained with the Cantor's Dust method as can be seen in Table 5. The spacing distribution of set 1 and set 4 do not show a power-law behavior and no clear linear section is seen. Figure 4 shows the spacing distribution of set 1 as an example.

6 DISCUSSION

Based on the Cantor's Dust method the intersections of different fracture sets with the Basel-1 borehole reveal fractal dimensions varying between 0.35 and 0.60.

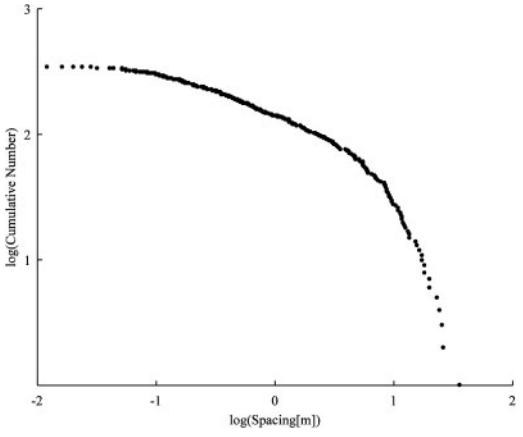

Figure 4. True spacing distribution of set 1, showing no evident power-law distribution.

Table 5. Power-law exponent of sets 2 and 3 compared with the fractal dimension given as 1–*D*.

Fracture set	Power-law exponent (|m|) [–]	1–*D* [–]
2	0.57	0.52
3	0.61	0.65

Low fractal dimensions (closer to zero) indicate highly clustered sets (sets 2 and 3), while higher values correspond to more evenly distributed fracture sets (sets 1 and 4). The fractal analysis of the three fracture sets (sets 1–3), occurring in the upper 400 m of the logged crystalline section, shows very similar fractal dimensions. This can be interpreted as same clustering behavior, which might reflect an influence of similar formation processes. At least, set 1 and set 2 may be a conjugate pair of tectonic fractures conform to the Hercynian direction (i.e., striking NW; Table 1). As discussed in section 4, the uppermost portion of the crystalline basement rocks has been exhumed close to the Earth's surface before Permian, Mesozoic and Cenozoic sedimentary rocks were deposited (Ziegler et al., 2015 and references therein). The fracture frequency distribution and p-wave velocities in this section are visibly different from the deeper parts of the penetrated crystalline basement. Different lithology, mechanical properties, rock texture and mineralogy, loading history etc., may lead to different distributions of fractures. Different fractal dimensions for different subintervals of the fracture set 3 might indicate such an effect with a stronger clustering possibly due to the overprint of near surface effects for the shallower interval (Table 3). However, the variation of fractal dimension with increasing depth for different sets is a topic for further investigations.

Although the statistical distribution of fracture sets is highly affected by censoring and truncation effects, power-law distributions were observed in two sets (sets 2 and 3) for about two orders of spacing magnitudes. We found that the exponents are very close to 1–*D*, with *D* previously obtained from Cantor's Dust analysis. Thus, it is possible to obtain the fractal dimension of a fracture set by using its statistical distribution if it follows a power-law.

7 CONCLUSIONS

The fractal dimension of different sets intersecting the Basel-1 geothermal well, utilizing the Cantor's Dust method, varies between 0.35 and 0.60. Low fractal dimensions correspond to low degree of clustering along the borehole. The fractal dimensions of three present sets in the first 400 m might reflect the same origin and fracture types. At least, set 1 and set 2 may be a conjugate pair of tectonic fractures. Different lithology, mechanical properties, rock texture and mineralogy, loading history etc., may lead to a different distribution of fractures. Moreover, the power-law exponent of the spacing distributions of two sets is very close to 1–*D*, obtained by Cantor's Dust analysis. It shows the possibility of obtaining the fractal dimension of fracture sets by using their statistical distributions (if these follow power-laws).

ACKNOWLEDGEMENTS

The research leading to these results has received funding from the European Community's Seventh Framework Program under grant agreement No. 608553 (Project IMAGE). A special gratitude is given to Dr. Keith Evans for his guidance and constructive criticism in performing this research.

REFERENCES

Barton, C. A. & Zoback, M. D. 1992. Self-similar distribution and properties of macroscopic fractures at depth in crystalline rock in the Cajon Pass Scientific Drill Hole. *Journal of Geophysical Research: Solid Earth (1978–2012)*, 97, 5181–5200.

Boadu, F. & Long, L. 1994. The fractal character of fracture spacing and RQD. International journal of rock mechanics and mining sciences & geomechanics abstracts. Elsevier, 127–134.

Bonnet, E., Bour, O., Odling, N. E., Davy, P., Main, I., Cowie, P. & Berkowitz, B. 2001. Scaling of fracture systems in geological media. *Reviews of Geophysics*, 39, 347–383.

Cantor, G. 1872. Über die Ausdehnung eines Satzes aus der Theorie der trigonometrischen Reihen. *Mathematische Annalen*, 5, 123–132.

Deere, D. & Deere, D. 1987. The rock quality designation (RQD) index in practice. Symposium on Rock Classification Systems for Engineering Purposes, Cincinnati, Ohio, USA, 1988.

Enescu, B. & Ito, K. 2001. Some premonitory phenomena of the 1995 Hyogo-Ken Nanbu (Kobe) earthquake: seismicity, b-value and fractal dimension. *Tectonophysics*, 338, 297–314.

Genter, A., Castaing, C., Dezayes, C., Tenzer, H., Traineau, H. & Villemin, T. 1997. Comparative analysis of

direct (core) and indirect (borehole imaging tools) collection of fracture data in the Hot Dry Rock Soultz reservoir (France). *Journal of Geophysical Research: Solid Earth (1978–2012)*, 102, 15419–15431.

Genter, A., Evans, K., Cuenot, N., Fritsch, D. & Sanjuan, B. 2010. Contribution of the exploration of deep crystalline fractured reservoir of Soultz to the knowledge of enhanced geothermal systems (EGS). *Comptes Rendus Geoscience*, 342, 502–516.

Hainzl, S. 2004. Seismicity patterns of earthquake swarms due to fluid intrusion and stress triggering. *Geophysical Journal International*, 159, 1090–1096.

Power, W. L. & Tullis, T. E. 1991. Euclidean and fractal models for the description of rock surface roughness. *Journal of Geophysical Research: Solid Earth (1978–2012)*, 96, 415–424.

Smalley, R., Chatelain, J.-L., Turcotte, D. & Prévot, R. 1987. A fractal approach to the clustering of earthquakes: applications to the seismicity of the New Hebrides. *Bulletin of the Seismological Society of America*, 77, 1368–1381.

Valley, B. 2007. *The relation between natural fracturing and stress heterogeneities in deep-seated crystalline rocks at Soultz-sous-Forêts (France).* Diss., Naturwissenschaften, Eidgenössische Technische Hochschule ETH Zürich, Nr. 17385.

Valley, B. & Evans, K. F. 2007. Stress state at Soultz-sous-Forêts to 5 km depth from wellbore failure and hydraulic observations. Proceedings, 32nd Workshop on Geothermal Reservoir Engineering. 17481–17469.

Valley, B. & Evans, K. F. 2009. Stress orientation to 5 km depth in the basement below Basel (Switzerland) from borehole failure analysis. *Swiss Journal of Geosciences*, 102, 467–480.

Velde, B., Dubois, J., Moore, D. & Touchard, G. 1991. Fractal patterns of fractures in granites. *Earth and Planetary Science Letters*, 104, 25–35.

Velde, B., Dubois, J., Touchard, G. & Badri, A. 1990. Fractal analysis of fractures in rocks: the Cantor's Dust method. *Tectonophysics*, 179, 345–352.

Ziegler, M., Valley, B. & Evans, K. F. 2015. Characterisation of Natural Fractures and Fracture Zones of the Basel EGS Reservoir Inferred from Geophysical Logging of the Basel-1 Well. Proceedings World Geothermal Congress, Melbourne, Australia, 19–25.